Supporting Information for

An Assessment of Antarctic Sea-ice Thickness in CMIP6 Simulations with Comparison to the Observations

Shreya Trivedi[1], Will Hobbs[2], and Marilyn Raphael[1]

[1]Department of Geography, University of California, Los Angeles

[2]Australian Antarctic Program Partnership, Institute for Marine and Antarctic Studies, University of Tasmania, nipaluna/Hobart, Australia.

Contents of this file

Introduction

The data files used in the supporting document are derived using Python. The format of the datasets was netcdf (.nc) format. The visualization generated is in the form of images (.png) format.

The anomaly time series have been produced by removing the climatological means from every timestep of the data for each sea-ice parameter i.e., Sea-ice Area, Thickness and Volume. These anomaly time-series were then segregated for two selected months in our study: *February* and *September* (Fig.S1) as well as four *austral* seasons (Fig.S2). We defined summer from December-February, Fall from March-May, Winter from June August, and Spring from September-November. Taylor diagram has been produced in Python using "*skill_metrics*" package. The spatial biases are calculated in Python by subtracting the observation dataset for respective months from the CMIP6 modeled data. (Fig.S4)

The reference data of sea-ice thickness is known to have exaggerated values especially for southern hemisphere.
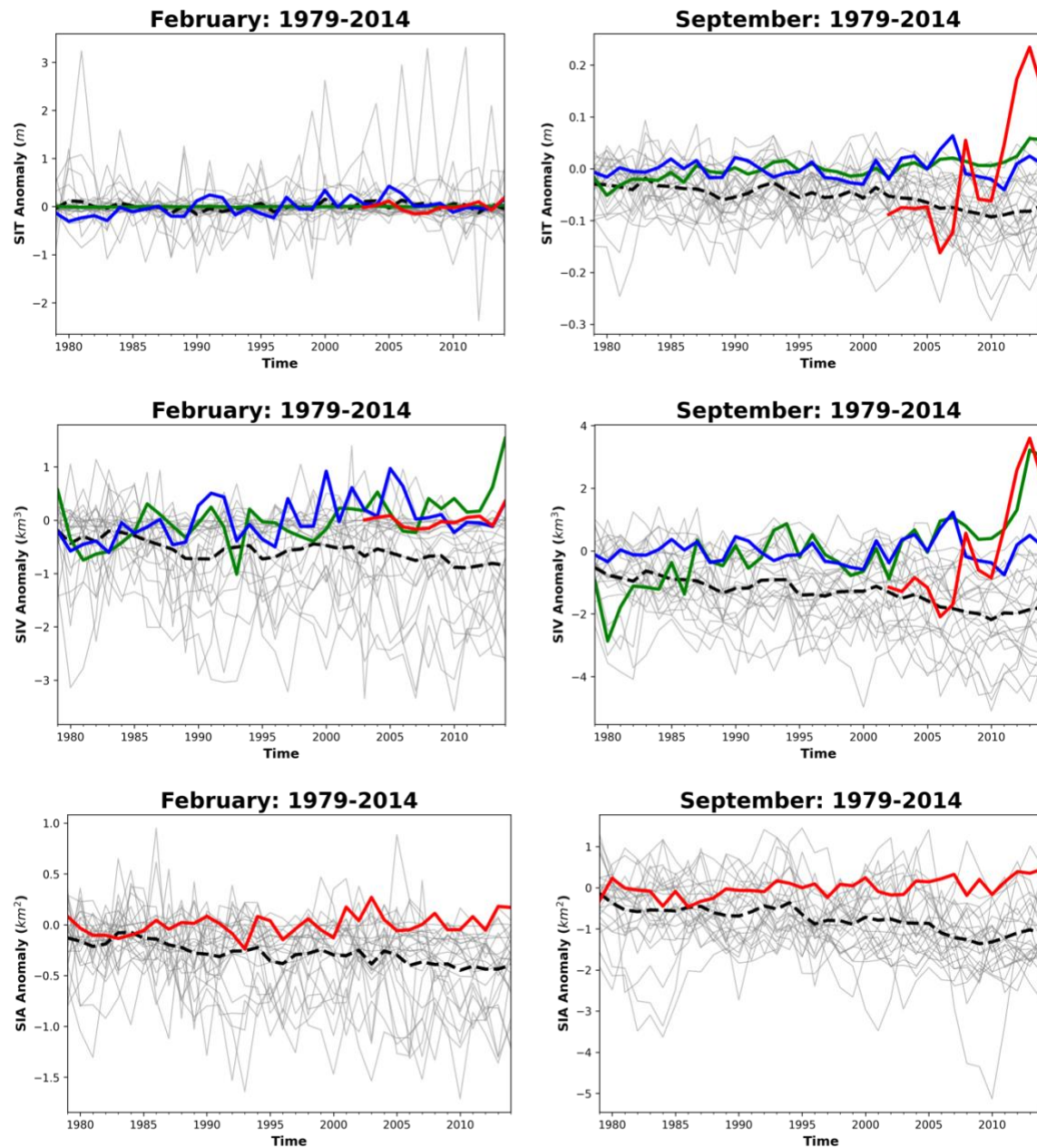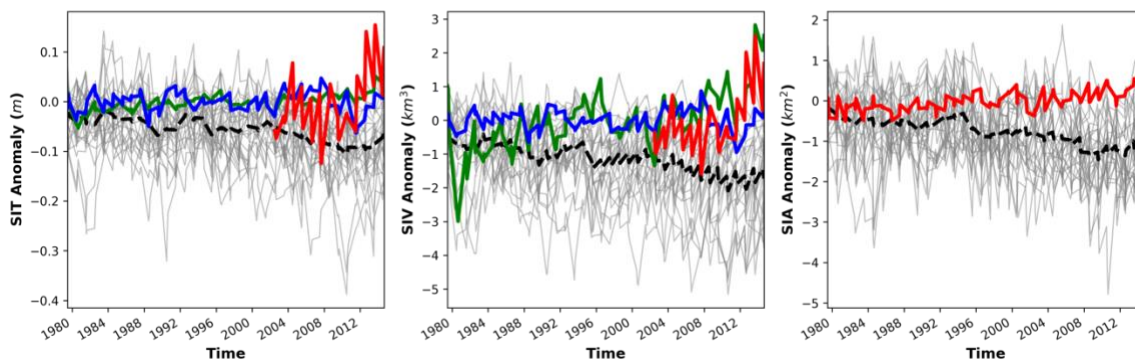
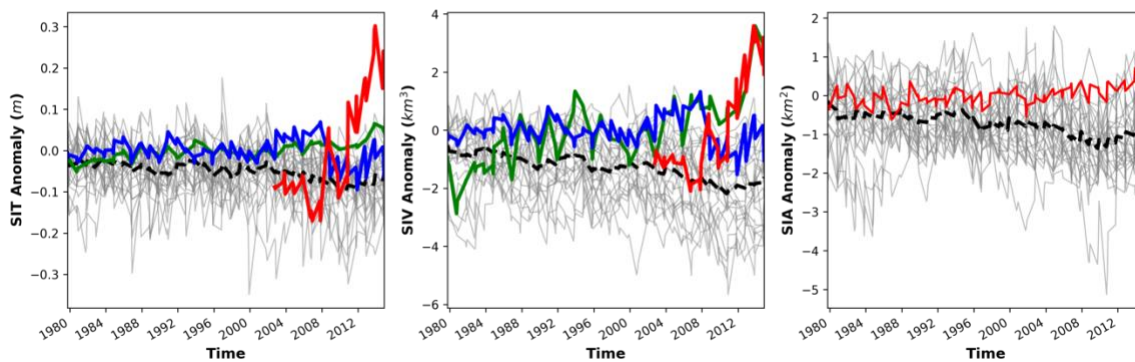**Figure S1:** Anomalies for the two months: **_February_** and **_September_** of sea-ice thickness (top), sea-ice volume (middle) and sea-ice area (bottom) of the circumpolar Antarctic. All the CMIP6 models are shown as grey lines, Multi-model mean in dashed line, GECCO3 in blue, GIOMASS in green, and Envisat-CryoSat-2/NSIDC in red.

Winter: 1979-2014

Spring: 1979-2014

Summer: 1979-2014

Fall: 1979-2014

3

Figure S2: Anomalies for four seasons: Spring and Winter (Colder Seasons), Summer and Fall (Warm Seasons) of sea-ice thickness (left), sea-ice volume (middle) and sea-ice area (right) of the circumpolar Antarctic. All the CMIP6 models are shown as grey lines, Multi-model mean in dashed line, GECCO3 in blue, GIOMASS in green, and Envisat-CryoSat-2/NSIDC in red.
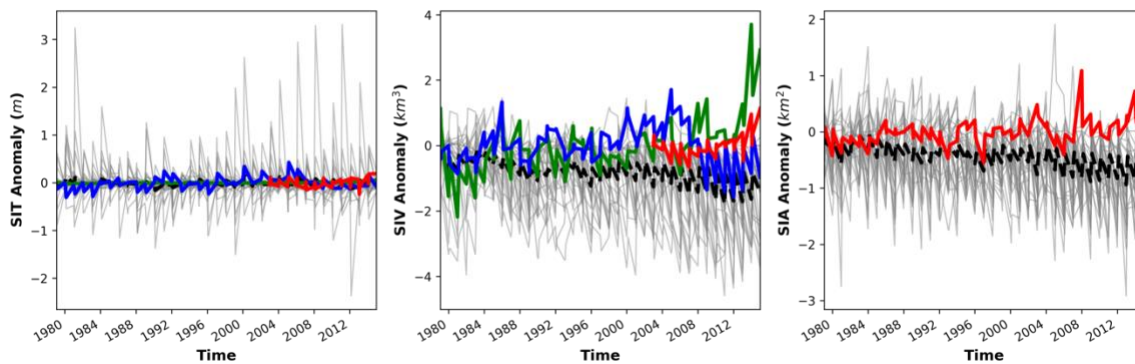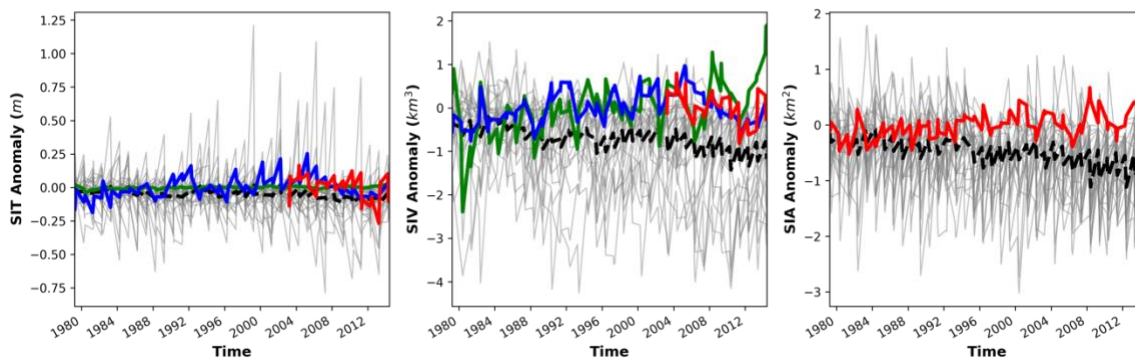

Figure S3: Taylor Diagrams representing spatial correlation using time-averaged means between CMIP6 models and different observation datasets where the distance between each model and the point labeled "Observed" is a measure of how realistically each model reproduces observations. For each model, three statistics are plotted: the Pearson correlation coefficient, related to the azimuthal angle (blue contours); the centered Root Mean Square Deviation (RMSD) in the simulated field viz proportional to the distance from the point on the x-axis identified as "observed" (green dashed contours); and the standard deviation of the simulated pattern viz proportional to the radial distance from

the origin (black dotted contours). Red dots represent individual CMIP6 models and black squares represent Reanalysis datasets. The period used for comparison is 2002-2014 for February (a,c,e) and September (b,d,f). For February, GECCO3 is not included as it had very small negative correlation. Reference datasets used for SIT and SIA are Envisat-CryoSat2 and NSIDC, respectively.

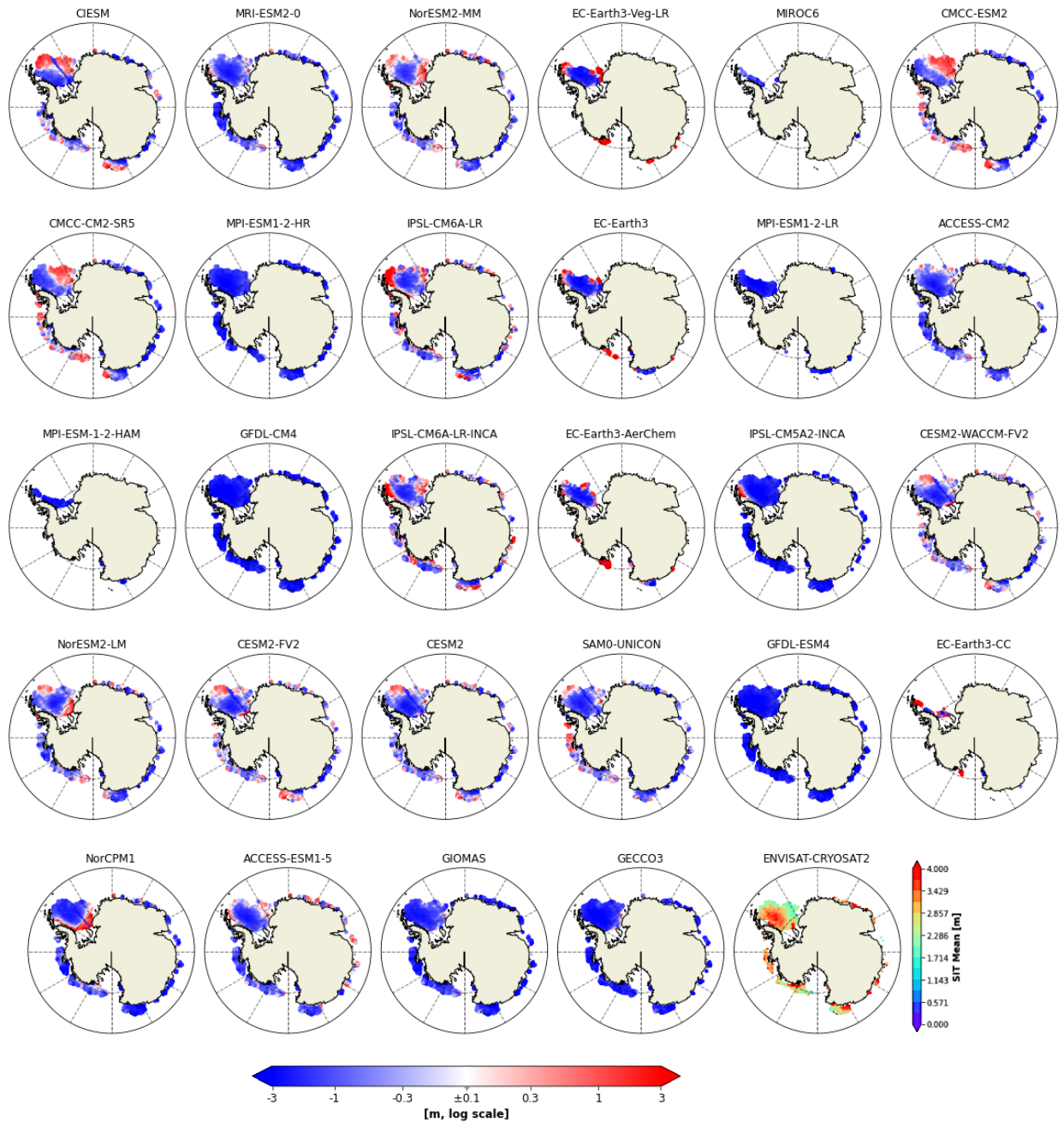**Fig. S4:** Spatial Biases of SIT from 2002 to 2014 *(February)* from 26 CMIP6 models and Reanalyses from the reference dataset: ENVISAT-CS-2. Last figure shows the time averaged SIT for ENVISAT-CS-2.

Model Name	Atmospheric Model	Ocean Model	Sea-Ice Model	References
ACCESS-CM2	MetUM-HadGEM3-GA7.1	ACCESS-OM2	CICE5.1.2	Dix et al., 2019
ACCESS-ESM1-5	HadGAM2 [250km]	ACCESS-OM2 (MOM5) [100km]	CICE4.1 [100km]	Ziehn et al., 2020
CESM2	CAM6 [100km]	POP2 [100km]	CICE5.1 [100km]	Danabasoglu et al., 2020
CESM2-FV2	CAM6 [100km]	POP2 [100km]	CICE5.1 [100km]	Danabasoglu et al., 2020
CESM2-WACCM-FV2	WACCM6	MAM4	CICE5.1	Danabasoglu et al., 2020, Gettelman et al., 2019
CIESM	CIESM-AM	CIESM-OM	CICE4	Lin et al., 2020
CMCC-CM2-SR5	CAM5.3	NEMO3.6	CICE4.0	Lovato et al., 2020
CMCC-ESM2	CAM5.3	NEMO3.6	CICE4.0	Cherchi et al., 2019
EC-Earth3	IFS cy36r4	NEMO3.6	LIM3	Massonnet et al., 2020
EC-Earth3-AerChem	IFS cy36r4	NEMO3.6	LIM3	van Noije et al., 2021
EC-Earth3-CC	IFS cy36r4	NEMO3.6	LIM3	Döscher et al., 2022
EC-Earth3-Veg-LR	IFS cy36r4 [100km]	NEMO3.6 [100km]	LIM3 [100km]	Wyser et al., 2020
GFDL-CM4	GFDL-AM4.0.1	GFDL-OM4p25	GFDL-SIM4p25	Held et al., 2019
GFDL-ESM4	GFDL-AM4.1	GFDL-OM4p5	GFDL-SIM4p5	Krasting et al., 2018
IPSL-CM5A2-INCA	LMDZ	NEMO-OPA	NEMO-LIM3	Boucher et al., 2020
IPSL-CM6A-LR-INCA	LMDZ	NEMO-OPA	NEMO-LIM3	Boucher et al., 2021
IPSL.IPSL-CM6A-LR	LMDZ [250km]	NEMO-OPA [100km]	NEMO-LIM3 [100km]	Lurton et al., 2020
MIROC6	CCSR AGCM	COCO4.9	COCO4.9	Tatebe et al., 2019
MPI-ESM-1-2-HAM	ECHAM6.3	MPIOM1.63	UNNAMED (thermodynamic (Semtner zero-layer) dynamic (Hibler 79)	Mauritsen et al., 2019
MPI-ESM1-2-HR	Same as above	Same as above	Same as above	Gutjahr et al., 2019
MPI-ESM1-2-LR	Same as above	Same as above	Same as above	Mauritsen et al., 2019

MRI-ESM2-0	MRI-AGCM3.	MRI.COM4.4	MRI.COM4.4	Yukimoto et al., 2019
NorCPM1	CAM-OSLO4.1	MICOM1.1	CICE4	Counillon et al., 2016
NorESM2-LM	CAM-OSLO	MICOM	CICE	Seland et al., 2020
NorESM2-MM	CAM-OSLO	MICOM	CICE	Seland et al., 2020
SAM0-UNICON	CAM5.3 with UNICON	POP2	CICE4.0	Park et al., 2019

Table S1: Details of the specifications of 26 CMIP6 models used in the study.

	February			September		
Models	**STD**	**RMSD**	**Corr**	**STD**	**RMSD**	**Corr**
ENV-CS2	1.021	0	1	1.269	0	1
ACCESS-CM2	0.777	0.326	0.903	0.534	0.642	0.847
NorCPM1	0.779	0.352	0.794	0.944	0.647	0.76
MPI-ESM-1-2-HAM	0.095	0.207	0.948	0.33	0.744	0.855
NorESM2-LM	1.507	0.498	0.789	1.267	0.769	0.613
MIROC6	0.135	0.193	0.982	0.34	0.652	0.777
MRI-ESM2-0	0.785	0.387	0.907	0.592	0.648	0.82
GFDL-ESM4	0.13	0.535	0.592	0.351	0.739	0.833
IPSL-CM5A2-INCA	0.323	0.502	0.471	0.503	0.725	0.702
EC-Earth3-CC	0.366	0.199	0.887	0.349	0.745	0.754
GFDL-CM4	0.117	0.544	0.517	0.379	0.716	0.862
NorESM2-MM	1.08	0.393	0.903	0.818	0.678	0.716
EC-Earth3-AerChem	0.626	0.217	0.81	0.489	0.709	0.792
CMCC-CM2-SR5	1.238	0.507	0.892	0.714	0.636	0.793
MPI-ESM1-2-HR	0.205	0.26	0.94	0.42	0.734	0.811
SAM0-UNICON	1.028	0.426	0.865	0.813	0.58	0.813
ACCESS-ESM1-5	1.012	0.39	0.896	0.704	0.655	0.758
CESM2-WACCM-FV2	1.281	0.57	0.693	0.966	0.707	0.677
EC-Earth3-Veg-LR	0.708	0.227	0.798	0.461	0.723	0.775
CESM2-FV2	1.417	0.655	0.655	1.134	0.779	0.607
EC-Earth3	0.634	0.226	0.823	0.446	0.725	0.777
CESM2	1.084	0.499	0.849	0.74	0.605	0.817
IPSL-CM6A-LR	1.603	0.395	0.809	0.914	0.59	0.8
MPI-ESM1-2-LR	0.185	0.262	0.93	0.362	0.755	0.834
CMCC-ESM2	1.233	0.494	0.891	0.679	0.626	0.811
CIESM	0.927	0.281	0.838	0.456	0.697	0.813
GIOMAS	0.675	0.487	0.041	0.515	0.699	0.226
GECCO3	0.876	0.478	-0.033	0.46	0.702	0.32

Table S2: Table showing spatial correlations, RMSDs and Standard Deviations for Sea-ice Thickness.

	February			September		
Models	**STD**	**RMSD**	**Corr**	**STD**	**RMSD**	**Corr**
ENV-CS2	0.592	0.000	1	0.760	0.000	1
ACCESS-CM2	0.301	0.263	0.567	1.070	0.536	0.77
NorCPM1	1.532	0.788	0.793	2.203	1.431	0.809
MPI-ESM-1-2-HAM	0.227	0.113	0.791	0.953	0.432	0.73
NorESM2-LM	1.357	0.325	0.547	1.417	0.528	0.687
MIROC6	0.057	0.120	0.578	0.673	0.393	0.596
MRI-ESM2-0	0.890	0.302	0.84	1.168	0.543	0.842
GFDL-ESM4	0.032	0.328	0.492	0.144	0.485	0.813
IPSL-CM5A2-INCA	1.933	1.228	0.375	3.234	2.280	0.657
EC-Earth3-CC	0.105	0.110	0.881	0.449	0.397	0.699
GFDL-CM4	0.008	0.337	0.423	0.042	0.548	0.848
NorESM2-MM	0.696	0.282	0.628	1.041	0.533	0.708
EC-Earth3-AerChem	0.338	0.143	0.772	0.682	0.383	0.752
CMCC-CM2-SR5	0.484	0.309	0.445	0.949	0.444	0.782
MPI-ESM1-2-HR	0.099	0.166	0.686	0.287	0.441	0.765
SAM0-UNICON	1.211	0.431	0.793	2.000	1.288	0.812
ACCESS-ESM1-5	1.045	0.349	0.695	1.557	0.869	0.657
CESM2-WACCM-FV2	1.520	0.665	0.57	2.007	1.049	0.753
EC-Earth3-Veg-LR	0.367	0.141	0.693	0.663	0.392	0.732
CESM2-FV2	1.868	0.845	0.531	2.284	1.216	0.713
EC-Earth3	0.437	0.146	0.727	0.657	0.395	0.727
CESM2	0.922	0.315	0.688	1.722	0.867	0.82
IPSL-CM6A-LR	0.895	0.263	0.767	1.442	0.741	0.743
MPI-ESM1-2-LR	0.457	0.153	0.707	1.168	0.491	0.794
CMCC-ESM2	0.385	0.307	0.459	0.907	0.408	0.807
CIESM	0.147	0.274	0.291	1.107	0.535	0.782
GIOMAS	0.432	0.287	0.102	0.334	0.418	0.301
GECCO3	0.566	0.292	-0.074	0.297	0.424	0.368

Table S3: Table showing spatial correlations, RMSDs and Standard Deviations for Sea-ice Volume. The STD and RMSD values are of scale 10^9m.

	February			September		
Models	**STD**	**RMSD**	**Corr**	**STD**	**RMSD**	**Corr**
NSIDC	0.200	0.000	1	0.288	0.000	1
ACCESS-CM2	0.130	0.121	0.488	1.031	0.742	0.787

NorCPM1	0.590	0.312	0.86	1.331	0.933	0.901
MPI-ESM-1-2-HAM	0.107	0.134	0.151	1.141	0.901	0.617
NorESM2-LM	0.171	0.116	0.551	0.676	0.458	0.742
MIROC6	0.015	0.126	0.05	0.555	0.461	0.39
MRI-ESM2-0	0.383	0.213	0.836	1.139	0.778	0.901
GFDL-ESM4	0.037	0.115	0.52	0.218	0.131	0.848
IPSL-CM5A2-INCA	0.608	0.480	0.464	3.415	2.705	0.797
EC-Earth3-CC	0.016	0.126	0.097	0.526	0.396	0.588
GFDL-CM4	0.009	0.125	0.466	0.061	0.195	0.866
NorESM2-MM	0.162	0.110	0.613	0.711	0.478	0.772
EC-Earth3-AerChem	0.076	0.124	0.287	0.687	0.483	0.717
CMCC-CM2-SR5	0.106	0.114	0.459	0.761	0.511	0.81
MPI-ESM1-2-HR	0.051	0.121	0.277	0.320	0.162	0.825
SAM0-UNICON	0.542	0.267	0.824	1.250	0.899	0.887
ACCESS-ESM1-5	0.339	0.195	0.684	1.047	0.758	0.779
CESM2-WACCM-FV2	0.387	0.237	0.723	1.175	0.866	0.864
EC-Earth3-Veg-LR	0.077	0.124	0.285	0.681	0.480	0.724
CESM2-FV2	0.394	0.235	0.719	1.195	0.862	0.874
EC-Earth3	0.085	0.125	0.302	0.661	0.470	0.691
CESM2	0.332	0.203	0.693	1.189	0.871	0.864
IPSL-CM6A-LR	0.186	0.108	0.713	0.953	0.629	0.786
MPI-ESM1-2-LR	0.211	0.174	0.293	1.510	1.156	0.748
CMCC-ESM2	0.097	0.114	0.454	0.769	0.517	0.811
CIESM	0.065	0.125	0.225	1.050	0.802	0.785
GIOMAS	0.213	0.000	0.761	0.190	0.000	0.943
GECCO3	0.187	0.000	0.682	0.090	0.000	0.936

Table S4: Table showing spatial correlations, RMSDs and Standard Deviations for Sea-ice Area. The STD and RMSD values are of scale 10^9m.